

Fast Reference Based MRI

L. Weizman¹, Y. C. Eldar¹, A. Eilam¹, S. Londner¹, M. Artzi² and D. Ben Bashat²

Abstract—In many clinical MRI scenarios, existing imaging information can be used to significantly shorten acquisition time or improve Signal to Noise Ratio (SNR). In those cases, a previously acquired image can serve as a reference image, that may exhibit similarity in some sense to the image being acquired. Examples include similarity between adjacent slices in high resolution MRI, similarity between various contrasts in the same scans and similarity between different scans of the same patients. In this paper we present a general framework for utilizing reference images for fast MRI. We take into account that the reference image may exhibit low similarity with the acquired image and develop a hybrid adaptive-weighted approach for sampling and reconstruction. Experiments demonstrate the performance of the method in three different clinical MRI scenarios: SNR improvement in high resolution brain MRI, utilizing similarity between T2-weighted and fluid-attenuated inversion recovery (FLAIR) for fast FLAIR scanning and utilizing similarity between baseline and follow-up scans for fast follow-up scanning.

Index Terms—Compressive sensing and sampling, Magnetic resonance imaging (MRI), Brain

I. INTRODUCTION

MRI is the method of choice for clinical brain imaging, as it involves no exposure to ionizing radiation and provides high quality of soft tissue imaging. However, the scanning procedure is relatively slow due to fundamental physical limitations. Many approaches have been developed to speed-up MRI acquisition based on partial sampling of the k-space.

Some of these methods utilize existing prior information to improve MRI reconstruction from undersampled data or use a reference image to improve reconstruction. State-of-the-art examples consist of imaging of contrast agent uptake [1] and dynamic MRI [2]. Since the introduction of Compressed Sensing (CS) to the field of MRI [3], the use of a reference image has been embedded also in a CS framework, such as in rapid dynamic MRI [4], [5].

We note, however, that there are many clinical imaging scenarios in which supplemental imaging information is neglected due to its low fidelity. For instance, in almost every clinical scanning protocol both T2-weighted and fluid-attenuated inversion recovery (FLAIR) contrasts are fully sampled, although they exhibit similarities in regions with low fluid concentration. In addition, the acquisition time a brain follow-up scan may be shortened if we know how to properly utilize existing previous scans of the same patient.

Reference based MRI can also be used when multiple repetitions are required to improve Signal to Noise Ratio (SNR). In many high resolution MRI applications, acquisition

has to be repeated several times for adequate SNR obtained via averaging. Here, a high SNR, low resolution image can be used as a reference to improve the quality of low SNR, high resolution images, thereby saving scanning time with no need for data undersampling. Besides being distinct from existing undersampling-based MRI approaches, this application can be used with conventional pulse sequences and therefore requires no pulse sequence programming for implementation.

An important point to account for in reference based MRI is that the level of similarity to the reference scan depends on the object being acquired. Therefore, this uncertainty has to be embedded in the acquisition and reconstruction approach.

The aim of this paper is to introduce a general framework for fast reference based MRI. In our framework, we allow the reference image to exhibit differences in noise level or some spatial regions versus the acquired image, and adjust the reconstruction and acquisition approaches accordingly. Experimental results demonstrate the applicability of the proposed method in three different scenarios that utilize similarity to a reference image. The first application exploits similarity between adjacent slices to improve SNR. The second application exploits similarity between two imaging contrasts for fast scanning of one of them, and the third application exploits similarity between different scans of the same patient for fast scanning of follow-up scans.

II. METHOD

We denote by $\mathbf{x} \in \mathbb{C}^N$ the N-pixel 2D complex image to be reconstructed, represented as a vector, $\mathbf{y} \in \mathbb{C}^M$ denotes the k-space measurements and \mathbf{F}_u is the undersampled Fourier transform operator. In addition, we assume that a reference scan, spatially matched to \mathbf{x} and denoted as \mathbf{x}_0 , is available.

In conventional reference based MRI, the reference scan is utilized by formalizing an optimization problem that takes into account the fidelity of the measurements and the similarity to the reference scan:

$$\min_{\mathbf{x}} \|\mathbf{F}_u \mathbf{x} - \mathbf{y}\|_2^2 + \lambda \|\mathbf{x} - \mathbf{x}_0\|_1 \quad (1)$$

where λ is a properly chosen regularization parameter. This optimization problem assumes high degree of similarity between \mathbf{x}_0 and \mathbf{x} , and is therefore suitable for very specific MRI applications, such as dynamic MRI.

We would like to introduce a general framework for reference based MRI, that also takes into account that \mathbf{x}_0 may exhibit differences versus \mathbf{x} . We formalize an optimization problem that enforces sparsity in both transform domain of \mathbf{x} and difference with respect to \mathbf{x}_0 :

$$\min_{\mathbf{x}} \|\mathbf{A}(\mathbf{F}_u \mathbf{x} - \mathbf{y})\|_2^2 + \lambda_1 \|\mathbf{W}_1 \Psi \mathbf{x}\|_1 + \lambda_2 \|\mathbf{W}_2(\mathbf{x} - \mathbf{x}_0)\|_1 \quad (2)$$

*This work was supported by the Ministry of Science and by the ISF I-CORE joint research center of the Technion and the Weizmann Institute, Israel. Corresponding author: weizmanl@tx.technion.ac.il

¹Department of EE, Technion, Haifa, Israel.

²Sourasky Medical Center, Tel-Aviv, Israel

where Ψ is a sparsifying transform operator, chosen as a wavelet transform in this paper, and \mathbf{A} controls the weight given to the fidelity of certain measurements (used to prioritize samples with high SNR). The matrices \mathbf{W}_1 and \mathbf{W}_2 are weighting matrices, $\mathbf{W}_k = \text{diag}([w_k^1, w_k^2, \dots, w_k^N])$ with $0 \leq w_k^i \leq 1$, that control the weight given to each element in the sparse representation. In particular, \mathbf{W}_2 is used to weight image regions according to their similarity level with the reference scan. The parameters λ_1 and λ_2 are regularization parameters that control the weight given to each term in the optimization problem.

The matrix \mathbf{A} plays an important role in cases where we the acquired data, \mathbf{y} consists of more than one image. In those cases, we give higher weights to images with higher SNR, based on the expected images' SNR estimated by the scanner. However, the weighting matrices \mathbf{W}_1 and \mathbf{W}_2 have to be determined during the acquisition process as described below.

Adaptive-Weighted reference based MRI

We propose a hybrid sampling-reconstruction mechanism that adapts itself to the actual similarity between the reference and the current scan. Adjusting the values of \mathbf{W}_1 and \mathbf{W}_2 , as well as the optimal sampling locations in the k-space is performed in an iterative manner, inspired by Weighted-CS [6] and adaptive sampling [7]. In each iteration, a few k-space samples are acquired, and $\hat{\mathbf{x}}$ is estimated, to serve as the basis for estimating the weighting matrices and the sampling pattern in the next iteration.

Our rationale behind the iterative computation of \mathbf{W}_k is as follows. For \mathbf{W}_1 , and under the assumption that \mathbf{x}_0 exhibits major differences versus \mathbf{x} , we would avoid embedding reference-based knowledge, i.e., $\mathbf{W}_1 \rightarrow \mathbf{I}$. Otherwise, we would like to relax the demand for sparsity on the elements in \mathbf{x} known to be in the support of \mathbf{x}_0 in its wavelet representation. For \mathbf{W}_2 , we would like to enforce sparsity only in spatial regions where $\mathbf{x} \approx \mathbf{x}_0$. To obtain these goals, the elements of the weighting matrices are defined as follows:

$$w_1^i = \begin{cases} 1, & \frac{||\Psi(\hat{\mathbf{x}} - \mathbf{x}_0)||_i}{1 + ||\Psi(\hat{\mathbf{x}} - \mathbf{x}_0)||_i} > \epsilon \\ \frac{1}{1 + ||\Psi\mathbf{x}_0||_i}, & \text{otherwise,} \end{cases} \quad (3)$$

$$w_2^i = \frac{1}{1 + ||\hat{\mathbf{x}} - \mathbf{x}_0||_i} \quad (4)$$

where $[\cdot]_i$ denotes the i th element of the vector in brackets and ϵ is a threshold for similarity in the sparse transform domain.

As to the random sampling pattern used in our approach, we utilize our prior knowledge in the formulation of the probability density function (pdf) from which the random sample locations are taken [7]. If we assume 2D Cartesian sampling of n k-space rows, $-\frac{n}{2} < k_y \leq \frac{n}{2}$, then the samples for each subsequent iteration are taken randomly according to the pdf $f_S(k_y)$ given below in (5). This pdf takes into account both variable density random sampling $f_{VD}(k_y)$ [3], and the

distribution of the reference image k-space data $f_R(k_y)$:

$$f_S(k_y) = \gamma f_R(k_y) + (1 - \gamma) f_{VD}(k_y) \\ f_R(k_y) = \frac{g_R(k_y)}{\sum_{k_y} g_R(k_y)}, \quad g_R(k_y) = \sum_{i \in k_y} [|\mathbf{F}\mathbf{x}_0|]_i \quad (5)$$

where \mathbf{F} indicates the $N \times N$ Fourier matrix, f_{VD} is a polynomial density of order 4 [3] and γ is the fidelity we give to the similarity between the current and the reference image. In this manner, the pdf used for random sampling matches the real distribution of the data, if the reference scan and the current scan exhibit high degree of similarity.

The proposed algorithm is coined Adaptive-Weighted Reference Based MRI and is summarized in Algorithm 1. We use SFISTA [8] to solve the ℓ_1 -minimization problem in the weighted reconstruction phase.

Algorithm 1 Adaptive-Weighted Reference Based MRI

Input:

Number of k-space samples acquired at each iteration: N_k ;
Number of iterations: L ; Reference image: \mathbf{x}_0 ;
Expected fidelity of measurements: \mathbf{A}

Output: Estimated image: $\hat{\mathbf{x}}$

Initialize:

$\mathbf{y} = \mathbf{0}$; $\mathbf{F}_u = \mathbf{0}$; $S = \emptyset$; $\mathbf{W}_1 = \mathbf{I}$, $\mathbf{W}_2 = \mathbf{0}$
Randomly define N_k k-space sampling locations: $S^{(1)}$

Sampling and reconstruction:

for $l = 1$ to L **do**

$S \leftarrow S \cup S^{(l)}$

Define undersample operator, $\mathbf{F}_u^{(l)}$ for locations in S .

Sample: $\mathbf{y}^{(l)} = \mathbf{F}_u^{(l)} \mathbf{x}$

Update: $\mathbf{y} = \mathbf{y} + \mathbf{y}^{(l)}$; $\mathbf{F}_u = \mathbf{F}_u + \mathbf{F}_u^{(l)}$

Weighted reconstruction: Estimate $\hat{\mathbf{x}}$ by solving (2)

Adaptive sensing: Update \mathbf{W}_1 and \mathbf{W}_2 (3)

Randomly define N_k samples, $S^{(l+1)}$, using pdf in (5)

end for

III. EXPERIMENTAL RESULTS

To demonstrate the performance of our reference based MRI approach we examine three MRI applications, all of which utilize a reference scan for improved reconstruction. In all experiments, partial k-space acquisition was obtained by down-sampling a fully sampled k-space. A Daubechies 4 wavelet transform was used as the sparsifying transform. Different values of λ_1, λ_2 in the range of [0.001, 0.9] were examined, and the best result in terms of image quality is presented in each case. All scans were performed on a GE Signa 1.5T HDx scanner. High SNR images reconstructed from fully sampled data serve as gold standard. The source code and data required to reproduce the results presented in this paper can be downloaded from:

<http://www.technion.ac.il/~weizman1/software>

A. Utilizing similarity between adjacent slices

In MRI, SNR is proportional to the number of protons involved in generating the measured signal. As a result, thick

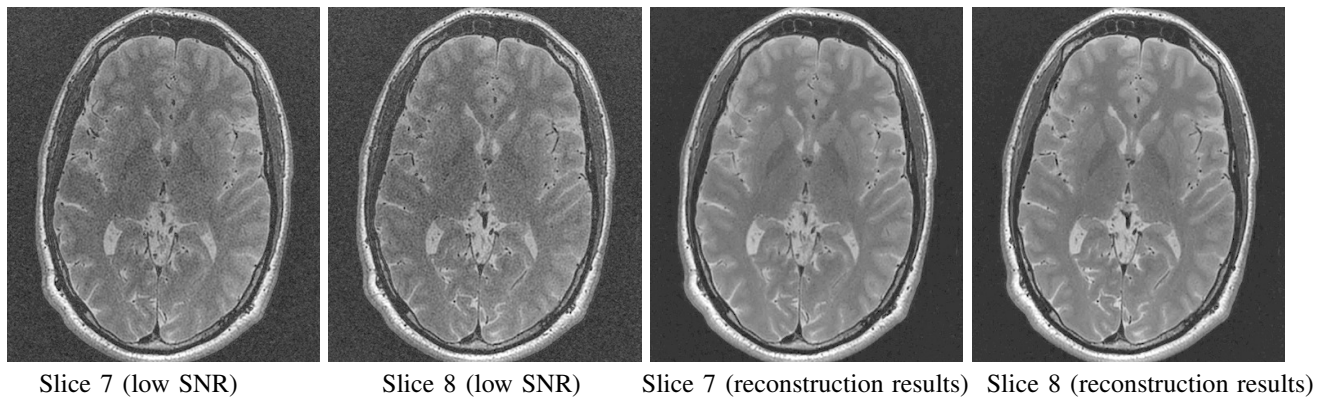


Fig. 1. Reference based MRI used within the same imaging contrast: reconstruction results from low SNR data. The two leftmost images show two adjacent T2-weighted slices acquired with a single repetition, and therefore have low SNR. It can be seen that these slices exhibit high similarity which can be exploited to improve SNR. The two rightmost images show the results of our reference-based method, obtained by exploiting similarity of thin slices and a high SNR thick slice (not shown). It can be seen that SNR is significantly improved.

slices provide better SNR than thin ones. To provide high SNR in 3D scans consisting of thin slices, scanning has to be repeated and averaged over several repetitions [9]. In this application we acquired a brain T2-weighted scan with slice thickness of 0.8mm followed by an additional acquisition with slice thickness of 1.6mm . In all scans a single repetition was used and the in plane resolution was $0.8 \times 0.8\text{mm}^2$. As a result, we obtained low SNR scan consisting of thin slices, and high SNR scan consisting of thick slices where each thick slice overlaps two thin ones. Our goal is to reconstruct a high SNR scan comprised of thin slices from this data.

Here, we assume that adjacent thin slices with no gap exhibit high degree of similarity and therefore we set $\mathbf{W}_2 = \mathbf{I}$. For simplicity, we use no adaptive sampling here and set $\mathbf{W}_1 = \mathbf{I}$. In addition, each thick slice spatially matches two adjacent thin (low SNR) slices. In this case, $\mathbf{y} = [y_1, y_2, y_3]^T$ represents the k-spaces of two thin slices and the corresponding thick one, respectively. Since a thick slice consists of averaged values of the thin ones, we denote $\mathbf{x} = [x_1, x_2, 0.5(x_1 + x_2)]^T$, where x_1 and x_2 are two adjacent thin slices. The matrix \mathbf{A} is determined by the estimated SNR of the elements in \mathbf{y} , giving higher values for elements corresponding to y_3 versus elements that correspond to y_1 and y_2 . Similarity is enforced between the thin slices, and (2) is reformulated to:

$$\min_{\mathbf{x}} \|\mathbf{A}(\mathbf{F}\mathbf{x} - \mathbf{y})\|_2^2 + \lambda_1 \|\Psi\mathbf{x}\|_1 + \lambda_2 \|(\mathbf{x}_1 - \mathbf{x}_2)\|_1. \quad (6)$$

Figure 1 shows two low SNR thin slices and their corresponding reconstruction results. In terms of scanning time, 4 repetitions are required to obtain thin slices with SNR comparable to SNR of data reconstructed with our method, yielding a speed-up factor of 2.6 for the proposed approach.

B. Utilizing similarity between T2-weighted and FLAIR

T2-weighted and FLAIR contrasts exhibit high similarity in non-fluid regions. In this case, our goal is to reconstruct the FLAIR image, \mathbf{x} , from undersampled measurements, utilizing this similarity. Images were acquired with in-plane resolution of $0.5 \times 0.5\text{mm}^2$ and with slice thickness of 4mm . We sampled

only 15% of the FLAIR k-space with variable density random sampling and utilized a fully sampled T2-weighted scan as the reference image (\mathbf{x}_0). Since all samples were acquired with similar SNR, $\mathbf{A} = \mathbf{I}$ and for simplicity we use no adaptive sampling and set $\mathbf{W}_1 = \mathbf{I}$. The values of \mathbf{W}_2 are chosen to be 0 for elements corresponding to pixels with high fluid concentration and 1 otherwise. The regions with high fluid concentration can be easily detected by their high intensity values in the reference image.

Figure 2 shows the fully sampled T2 and FLAIR images, reconstruction based on sparsity in wavelet domain only, and our reference based reconstruction. It can clearly be seen that reference-based FLAIR reconstruction outperforms traditional wavelet sparsity based FLAIR reconstruction, using only 15% of the data.

C. Utilizing similarity between baseline of follow-up scans

Repeated brain MRI scans of the same patient every few weeks or months are very common for follow-up of brain tumors [10], [11]. Here, our goal is to use a previous scan in the time series as a reference scan for reconstruction of a follow-up scan. In this application we need to tackle problems that do not exist in previous applications described in this paper, such as grey-level variations and miss-registration between scans acquired at different dates. While these obstacles can be addressed by grey-level normalization and reproducing the same slices position in the follow-up scan [12], similarity between the reference and current scans is not still not guaranteed, and prior information on spatial regions that may exhibit differences is not available.

Therefore, in this case we used all the features described in Section II and estimated \mathbf{W}_1 and \mathbf{W}_2 in an adaptive manner. The threshold for defining similarity in the sparse transform domain was set to $\epsilon = 0.1$. Since \mathbf{W}_2 serves as a good approximation for the actual degree of similarity between scans, the value of γ in (5) was computed as $\gamma = \frac{1}{N} \sum_{i=1}^N w_i^2$ in each iteration. Since all samples were acquired with similar SNR, we set $\mathbf{A} = \mathbf{I}$.

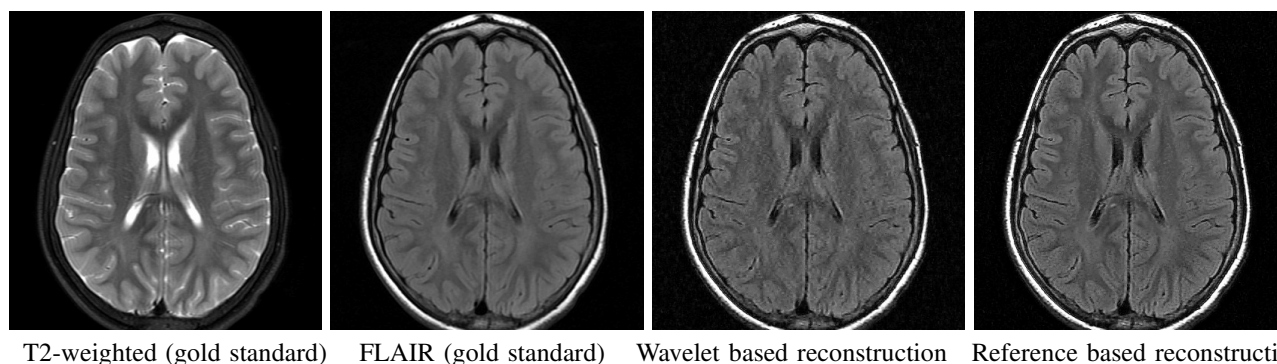


Fig. 2. Reference based MRI used within the same scan: reconstruction results utilizing similarity between T2 and FLAIR contrasts. The similarity between T2 and FLAIR in regions with low fluid concentration (demonstrated in the two leftmost images) is utilized for high quality reconstruction from 15% of k-space FLAIR data (rightmost image). State-of-the-art wavelet based reconstruction using the same data results in imaging artifacts (second from right).

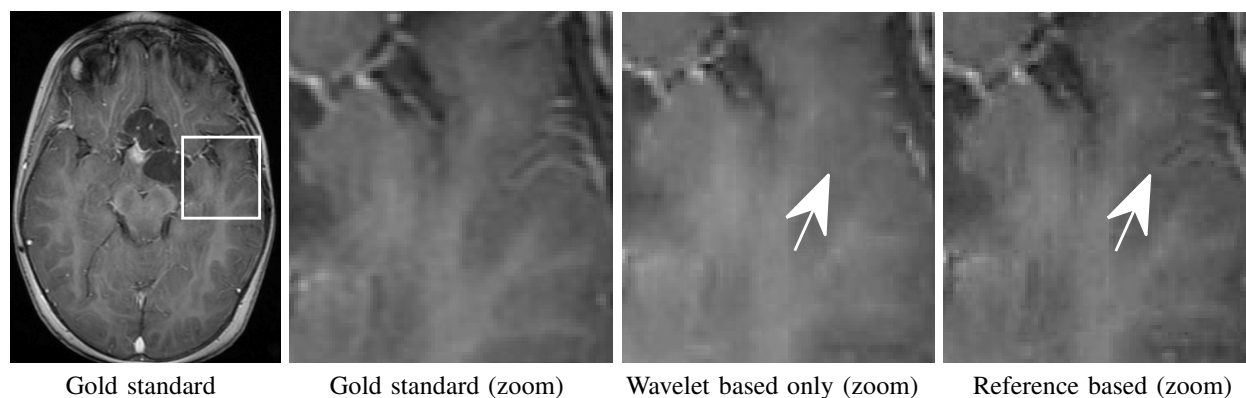


Fig. 3. Reference based MRI used in longitudinal studies: reconstruction results from 6% of k-space data. The enlarged region shown the three rightmost images corresponds to the marked region in the leftmost image. It can be seen that our reference-based approach exhibits results which are very similar to the gold standard, and reveals imaging features that are not visible in state-of-the-art wavelet based MRI reconstruction.

Figure 3 shows reconstruction results of a follow-up T1-weighted brain scan utilizing the baseline scan as a reference scan (resolution: $0.5 \times 0.5 \text{mm}^2$, thickness: 1mm for both scans). Results were obtained using only 6% of k-space data. It can be seen that the reference based method exhibits imaging features that are hardly visible in the wavelet based reconstruction method. The superiority of our approach is achieved thanks to its hybrid mechanism that adapts the sampling and reconstruction during scanning.

IV. CONCLUSIONS

In this paper we introduce a new framework for reference based MRI. We developed a hybrid sampling and reconstruction approach that supports cases in which similarity to the reference scan is not guaranteed. We demonstrate the performance of our approach in three clinical MRI applications, including reconstruction from noisy images and from undersampled k-space data. Results exhibit significant improvement versus wavelet sparsity based MRI. Thanks to the existence of reference image in various clinical imaging scenarios, the proposed approach can play a major part in improving reconstruction in many MR applications.

REFERENCES

- [1] J. J. Van Vaals et al., "keyhole method for accelerating imaging of contrast agent uptake," *Journal of Magnetic Resonance Imaging*, vol. 3, no. 4, pp. 671–675, 1993.
- [2] C. A. Mistretta et al., "Highly constrained backprojection for time-resolved MRI," *Magn. Res. Med.*, vol. 55, no. 1, pp. 30–40, 2006.
- [3] M. Lustig et al., "Sparse MRI: The application of compressed sensing for rapid MR imaging," *Magnetic resonance in medicine*, vol. 58, no. 6, pp. 1182–1195, 2007.
- [4] F. Lam et al., "Compressed sensing reconstruction in the presence of a reference image," in *Proc. 18th ISMRM*, 2010, vol. 18, pp. 4861–4861.
- [5] Huiqian Du and Fan Lam, "Compressed sensing mr image reconstruction using a motion-compensated reference," *Magnetic resonance imaging*, vol. 30, no. 7, pp. 954–963, 2012.
- [6] E. J. Candes et al., "Enhancing sparsity by reweighted l1 minimization," *J. of Fourier analysis and applications*, vol. 14, pp. 877–905, 2008.
- [7] Y. Chen et al., "Completing any low-rank matrix, provably," *arXiv preprint arXiv:1306.2979*, 2013.
- [8] Z. Tan et al., "Smoothing and decomposition for analysis sparse recovery," *IEEE Trans. on Sig. Proc.*, vol. 62, pp. 1762–1774, 2014.
- [9] L. Weizman et al., "Exploiting similarity in adjacent slices for compressed sensing MRI," in *Proc. of EMBC*, 2014, pp. 1549–1552.
- [10] L. Weizman et al., "Automatic segmentation and components classification of optic pathway gliomas in MRI," in *MICCAI 2010*, pp. 103–110. Springer, 2010.
- [11] L. Weizman et al., "The application of compressed sensing for longitudinal MRI," *arXiv preprint arXiv:1407.2602*, 2014.
- [12] K. McMillan et al., "MR efficiency becomes critical as healthcare costs, scanner time demand increases," *Signa Pulse of MRI*, vol. Autumn 2010, pp. S10–S13, 2010.